Method for calculating the heat and momentum fluxes of inhomogeneous fluids

Minsub Han
Micro Thermal Research Center, Seoul National University, Seoul, Korea

Joon Sik Lee
School of Mechanical and Aerospace Engineering, Seoul National University, Seoul, Korea

(Received 10 June 2004; published 29 December 2004)

We present a method for calculating the heat and momentum fluxes of general fluids away from equilibrium. Our method is capable of resolving strongly inhomogeneous nonequilibrium flows, and applicable to three-dimensional problems. Our flux expressions correspond to the flux definitions originally suggested by Irving and Kirkwood [J. Chem. Phys. **18**, 817 (1950)] and are equivalent to the method of planes [Phys. Rev. E **48**, 4110 (1993)] used to calculate flow in a simple geometry. Nonequilibrium molecular dynamics simulations are performed showing that our method reveals a significant heat transfer in the upstream direction due to the so-called "*plane peculiar velocity*." In a general geometry, our method may resolve features such as stress concentration near edges and flux gradients parallel to the flow.

DOI: 10.1103/PhysRevE.70.061205 PACS number(s): 47.17.+e, 05.10.−a, 44.05.+e

I. INTRODUCTION

The flux of heat and momentum provides essential information in the understanding of fluid dynamic behavior, and there is growing interest in the properties of inhomogeneous fluids, which are fundamental to many nanosystems. These fluxes can be directly related to the microscopic constituents of a system, such as molecules, through the use of statistical mechanics. The virial approach provides an equation for the pressure of a homogeneous fluid [1]. A more direct approach, however, is to specify the mechanical contributions of the molecules to these fluxes, which originate from two different types of molecular action. One is the kinetic component, which comes from the transport of molecules, and the other the potential component, manifested through molecular interactions. Real fluid molecules, which have finite size and many-body interactions, are difficult to define clearly on the contributions. Even for a monatomic fluid that interacts through pairwise interactions, there is still a problem with the potential components. For a given infinitesimal area, we need to determine which pair contributes to the flux through the potential. The simplest choice would be a pair whose line of center meets at a point within the area of interest. Using this definition, Irving and Kirkwood derived hydrodynamic equations employing classical statistical mechanics and obtained expressions for the pressure tensor and heat flux vector of [2,3]

$$\mathbf{P}(\vec{r},t)=\left\langle \sum_{j=1}^{N} m(\vec{v}_j-\vec{u})(\vec{v}_j-\vec{u})\delta(\vec{r}_j-\vec{r}) - \frac{1}{2}\sum_{j}^{N}\sum_{k(\neq j)}^{N}\vec{r}_{jk}\vec{\mathbf{F}}_{jk}O_{jk}\delta(\vec{r}-\vec{r}_j);f\right\rangle, \tag{1a}$$

$$\vec{\mathbf{J}}(\vec{r},t)=\left\langle \sum_{j=1}^{N}(\vec{v}_j-\vec{u})U_j\delta(\vec{r}_j-\vec{r}) - \frac{1}{2}\sum_{j}^{N}\sum_{k(\neq j)}^{N}\vec{r}_{jk}(\vec{v}_j-\vec{u})\cdot\vec{\mathbf{F}}_{jk}O_{jk}\delta(\vec{r}-\vec{r}_j);f\right\rangle, \tag{1b}$$

where

$$U_j=\frac{1}{2}m|\vec{v}_j-\vec{u}(\vec{r}_j)|^2+\frac{1}{2}\sum_j\phi_{jk}, \tag{2}$$

and $\langle a;f\rangle$ represents the ensemble average of a with respect to the distribution function, f:

$$\langle a;f\rangle\equiv\int dr^{3N}dp^{3N}a(r^{3N},p^{3N},\vec{r})f(r^{3N},p^{3N},t).$$

The terms r^{3N} and p^{3N} represent the $3N$ coordinates and $3N$ momenta of the system, respectively. And O_{jk} is given by

$$O_{jk}=1-\frac{1}{2!}\vec{r}_{jk}\cdot\frac{\partial}{\partial\vec{r}}+\cdots+\frac{1}{n!}\left(-\vec{r}_{jk}\cdot\frac{\partial}{\partial\vec{r}}\right)^{n-1}+\cdots. \tag{3}$$

In the above equations, j, k are the indices of the particles, N is the total number of particles in the system, and m is the mass of the particles. The terms $\vec{v}_j$ and $\vec{r}_j$ are the velocity and position of particle j, respectively, $\vec{u}(\vec{r})$ is the streaming velocity at position $\vec{r}$, $\vec{r}_{jk}$ is the position of particle k relative to that of particle j, and $\vec{F}_{jk}$ is the intermolecular force that acts on particle k from particle j. The term ϕ_{jk} is the intermolecular potential. However, there is no unique definition of the potential contribution to the fluxes. For example, Harashima suggests that the molecules inside a prism contribute to the fluxes on the prism base area when they interact with any

molecule on the other side of the boundary surface that contains the base area [4]. There are also many other choices that all conform to the conservation equations [5]. However, the definition of Harashima may not be robust [6]. Another study proposed an additional criterion for a unique definition, which results in the expressions of Irving and Kirkwood [7].

Meanwhile, it can be seen that Eq. (1) requires the ensemble average. This results from the derivation of Eq. (1) where the mass, momentum, and energy densities are initially defined according to the ensemble average with respect to the distribution function. For example, the density is given by

$$\rho(\vec{r},t) = \sum_{j=1}^{N} \langle m\delta(\vec{r}_j - \vec{r}); f\rangle.$$

The procedure is, however, time consuming to implement in molecular simulations. Alternatively, expressions for the fluxes can be used to satisfy the conservation equations at any given instant for a defined system [3]

$$\mathbf{P}(\vec{r},t) = \sum_{j=1}^{N} m[\vec{v}_j(t) - \vec{u}(\vec{r},t)][\vec{v}_j(t) - \vec{u}(\vec{r},t)]\delta(\vec{r}_j(t) - \vec{r}) - \frac{1}{2}\sum_{j=1}^{N}\sum_{k=1(\neq j)}^{N} \vec{r}_{jk}\vec{\mathbf{F}}_{jk}O_{jk}\delta(\vec{r} - \vec{r}_j(t)), \tag{4a}$$

$$\vec{\mathbf{J}}(\vec{r},t) = \sum_{j=1}^{N} [\vec{v}_j(t) - \vec{u}(\vec{r},t)]U_j(t)\delta(\vec{r}_j(t) - \vec{r}) - \frac{1}{2}\sum_{j=1}^{N}\sum_{k=1(\neq j)}^{N} \vec{r}_{jk}(t)\vec{\mathbf{F}}_{jk}(t)\cdot[\vec{v}_j(t) - \vec{u}(\vec{r},t)] \times O_{jk}\delta(\vec{r} - \vec{r}_j(t)). \tag{4b}$$

These equations are based on the *instantaneous* density of the mass, momentum, and energy. For example, the density is given by

$$\rho(\vec{r},t) = \sum_{j=1}^{N} m\delta(\vec{r}_j - \vec{r}).$$

These expressions can be evaluated for a single system trajectory, which is particularly useful in molecular simulations. However, there remains a critical difficulty in evaluating the operator O_{jk} using these expressions. This operator acts on the delta function and produces an infinite sum of its derivatives. It becomes increasingly difficult to evaluate higher-order derivatives directly, which, on the other hand, may not decay fast enough to be neglected in an inhomogeneous fluid. Often found in the literature is an $O_{jk} \simeq 1$ approximation, which is valid only in the cases of homogeneous or weakly inhomogeneous fluids. Todd *et al.* overcame the above situation by adopting measures that include manipulation in the reciprocal space [8]. They introduced the so-called "*method of planes*" (MOP), which does not require evaluating O_{jk} [8–10]:

$$P_{y\alpha}(y) = \frac{1}{A}\left\{ \lim_{\tau\to\infty}\frac{1}{\tau}\sum_{0<t_{j,l}<\tau}\sum_{j=1}^{N} m[v_{\alpha j}(t_{j,l}) - u_\alpha(y)]\mathrm{sgn}[v_{yk}(t_{j,l})] - \frac{1}{4}\sum_{j=1}^{N}\sum_{k=1(\neq j)}^{N} F_{\alpha jk}[\mathrm{sgn}(y - y_j) - \mathrm{sgn}(y - y_k)]\right\}, \tag{5a}$$

$$J_y(y) = \frac{1}{A}\left\{ \lim_{\tau\to\infty}\frac{1}{\tau}\sum_{0<t_{j,l}<\tau}\sum_{j=1}^{N} U_j(t_{j,l})\mathrm{sgn}[v_{yk}(t_{j,l})] - \frac{1}{4}\sum_{j=1}^{N}\sum_{k=1(\neq j)}^{N} [\vec{v}_j - \vec{u}(y)]\cdot\vec{\mathbf{F}}_{jk}[\mathrm{sgn}(y - y_j) - \mathrm{sgn}(y - y_k)]\right\}. \tag{5b}$$

Here, A is the area of measurement, y is the coordinate for the direction normal to the flow, and α denotes x, y, or z. The term $t_{j,l}$ is the time when particle j crosses the plane l times during the time period τ, and sgn is the sign function.

However, the MOP is still limited in that it is derived from, and applicable only to, unidirectional flows. The flow direction needs to be tangential to the measurement surface, and only part of the flux components is provided: for example, P_{xx}, P_{xy}, or J_x are not given in terms of the coordinates used in Eq. (5). In addition, the flux gradients in the tangential direction to the measurement surface, for example, the x or z directions, are not considered in the derivation.

While the MOP is a valuable tool for probing many phenomena in inhomogeneous fluids, some problems inevitably involve the fluxes not resolved well using this method. For example, it may be necessary to resolve a flux that varies in more than one direction, or the gradient of a flux in the flow direction. One recent study used a method that measures the potential part of the pressure tensor in a similar manner to that used in this work [11]. The authors of the study, however, relied on physical arguments for introducing this approach. To the best of our knowledge, there has been no other study on this issue published in the literature.

We begin with the expressions for instantaneous fluxes, Eq. (4), and then we derive the pressure tensor and heat flux vector that not only accurately represent a strongly inhomogeneous fluid in nonequilibrium state, but also resolve the state in a general geometry. The first step is to replace the operator O_{jk} by a more manageable operator. The final expressions correspond to the original flux definition of Irving and Kirkwood. For the flow in a simple geometry, these are equivalent to the MOP. Section II is devoted to the derivation of the expressions for fluxes, which are evaluated for two types of nanoscale fluid flow channels in Sec. III. The final section contains our conclusions.

II. THEORETICAL MODELS FOR FLUXES

A. Alternative form of O_{jk}

In the original derivation of the pressure tensor by Irving and Kirkwood [2], the operator O_{jk} was introduced when the

two delta functions according to the positions of two particles were expanded using a given relative position. The first few terms of the expansion are relatively easy to evaluate, and are adequate to model homogeneous and weakly inhomogeneous fluids. However, the higher-order derivatives of the delta function are increasingly difficult to handle, and they are of a non-negligible size for highly inhomogeneous fluids. The situation may be relieved using an integrated form of the delta function, since this smoothes out the extreme behavior of the function. It is interesting to note that the integrated version of O_{jk} has already been used in Ref. [2]. Applying it to the delta function gives the following relationships:

$$\int_0^1 d\alpha\delta(\vec{r}-\vec{r}_j-\alpha\vec{r}_{jk}) = \left[1-\frac{1}{2!}\vec{r}_{jk}\cdot\frac{\partial}{\partial\vec{r}}+\ldots+\frac{1}{n!}\times\left(-\vec{r}_{jk}\cdot\frac{\partial}{\partial\vec{r}}\right)^{n-1}+\ldots\right]\delta(\vec{r}-\vec{r}_j) = O_{jk}\delta(\vec{r}-\vec{r}_j). \quad (6)$$

This can be checked easily from the fact that

$$\delta(\vec{r}-\vec{r}_j-\alpha\vec{r}_{jk}) = \left[1-\alpha\vec{r}_{jk}\cdot\frac{\partial}{\partial\vec{r}}+\ldots+\frac{\alpha^{n-1}}{(n-1)!}\times\left(-\vec{r}_{jk}\cdot\frac{\partial}{\partial\vec{r}}\right)^{n-1}+\ldots\right]\delta(\vec{r}-\vec{r}_j). \quad (7)$$

Therefore, the delta function acted on by O_{jk} can be replaced by an integrated form of the delta function [15,16]. Thus Eq. (4) can be rewritten as

$$\mathbf{P}(\vec{r},t) = \sum_{j=1}^{N} m(\vec{v}_j-\vec{u})(\vec{v}_j-\vec{u})\delta(\vec{r}_j-\vec{r}) - \frac{1}{2}\sum_{j}^{N}\sum_{k(\neq j)}^{N}\vec{r}_{jk}\vec{\mathbf{F}}_{jk}\int_0^1 d\alpha\delta(\vec{r}-\vec{r}_j-\alpha\vec{r}_{jk}), \quad (8a)$$

$$\vec{\mathbf{J}}(\vec{r},t) = \sum_{j=1}^{N}(\vec{v}_j-\vec{u})U_j\delta(\vec{r}_j-\vec{r}) - \frac{1}{2}\sum_{j}^{N}\sum_{k(\neq j)}^{N}\vec{r}_{jk}\vec{\mathbf{F}}_{jk}\cdot(\vec{v}_j-\vec{u})\int_0^1 d\alpha\delta(\vec{r}-\vec{r}_j-\alpha\vec{r}_{jk}), \quad (8b)$$

where the functional dependence on $\vec{r}$ and t of the variables on the right-hand side has been omitted. These representations of the fluxes have a major advantage over previous representations in that they enable a direct evaluation of the contribution without any truncation of the terms. In the following section, these are elaborated on further, to provide more accessible forms for calculations.

B. Pressure tensor and heat flux vector

As in the MOP approach, the fluxes were measured on a plane across which momentum and energy can be exchanged. This can be compared with measurements on a bin. The measured fluxes are averaged on the plane A_o of a finite area $\Delta A=\Delta r_\alpha\Delta r_\beta$ centered at $\vec{r}_o=(r_{o\alpha},r_{o\beta},r_{o\gamma})$ as

$$\tilde{\mathbf{G}}(\vec{r}_o,t) \equiv \langle\mathbf{G}(\vec{r},t)\rangle_{\Delta A} \equiv \frac{1}{\Delta A}\int_{r_{o\alpha}-\Delta r_\alpha/2}^{r_{o\alpha}+\Delta r_\alpha/2} dr_\alpha\int_{r_{o\beta}-\Delta r_\beta/2}^{r_{o\beta}+\Delta r_\beta/2} dr_\beta\mathbf{G}(\vec{r},t),$$

where α, β, and γ are the indices for the rectangular coordinates, and γ is chosen as the coordinate normal to the plane: for example, $r_\gamma=y$ in the coordinates of Eq. (5). The time average is also defined as

$$\hat{\mathbf{G}}(\vec{r}_o,t_o) \equiv \frac{1}{\tau}\int_{t_o-\tau/2}^{t_o+\tau/2} dt\,\tilde{\mathbf{G}}(\vec{r}_o,t).$$

First, the kinetic contribution to the pressure tensor, $\mathbf{P}^K$, was considered

$$\mathbf{P}^K(\vec{r},t) = \sum_{j=1}^{N} m[\vec{v}_j(t)-\vec{u}(\vec{r},t)][\vec{v}_j(t)-\vec{u}(\vec{r},t)]\delta[\vec{r}_j(t)-\vec{r}]. \quad (9)$$

In the form of components, this is

$$\mathbf{P}^K_{\gamma\alpha}(\vec{r},t) = \sum_{j=1}^{N} m(v_{j\alpha}-u_\alpha)(v_{j\gamma}-u_\gamma)\delta(r_{j\alpha}-r_\alpha)\delta(r_{j\beta}-r_\beta)\times\delta(r_{j\gamma}-r_\gamma).$$

The term $\mathbf{P}_{\gamma\alpha}$ represents the pressure tensor applied in the α direction on a plane normal to γ. The average on the plane gives

$$\tilde{\mathbf{P}}^K_{\gamma\alpha}(\vec{r}_o,t) = \frac{1}{\Delta A}\sum_{j=1}^{N} m[v_{j\alpha}(t)-u_\alpha(\vec{r}_o,t)][v_{j\gamma}(t)-u_\gamma(\vec{r}_o,t)]\Omega_o\delta(r_{j\gamma}(t)-r_{o\gamma}), \quad (10)$$

where Ω_o is defined as

$$\Omega_0 = \begin{cases} 1, & \text{if } r_{o\alpha}-\dfrac{\Delta r_\alpha}{2}<r_{j\alpha}<r_{o\alpha}+\dfrac{\Delta r_\alpha}{2} \quad \text{and} \quad r_{o\beta}-\dfrac{\Delta r\beta}{2}<r_{j\beta}<r_{o\beta}+\dfrac{\Delta r_\beta}{2}, \\ 0, & \text{otherwise.} \end{cases}$$

Next, an average of Eq. (10) may need to be taken to make it more accessible. A usual approach would be to take an average over a small, but finite, dimension, Δr_γ, or to use coarse graining in the extra space dimension. This approach is equivalent to the bin average. The average over the volume rather than the area can be avoided if coarse graining over time is adopted instead. This approach was originally adopted by MOP, but here it is extended to a more general geometry. For a particle j that crosses the plane once during a given time period, with a known position r_γ, fixed in space, it follows that

$$v_{j\gamma}(t)\,\delta(r_{j\gamma}(t)-r_\gamma)=\frac{1}{2}\frac{d}{dt}\mathrm{sgn}[r_{j\gamma}(t)-r_\gamma]$$
$$=\delta(t_j-t)\mathrm{sgn}[v_{j\gamma}(t)], \qquad (11)$$

where t_j is the time when particle j is at r_γ. For $v_{j\gamma}\neq 0$,

$$\delta(r_{j\gamma}(t)-r_j)=\delta(t_j-t)\frac{1}{|v_{j\gamma}(t)|}.$$

If particle j crosses plane A_o lth time at $t=t_{j,l}(t_o-\tau/2<t_{j,l}<t_o+\tau/2)$, then the time average of Eq. (10) over τ will be

$$\hat{\mathbf{P}}^K_{\gamma\alpha}(\vec{r}_o,t_o)=\frac{1}{\Delta A\tau}\sum_j\sum_{t_{j,l}} m[v_{j\alpha}(t_{j,l})-u_\alpha(\vec{r}_o,t_{j,l})]$$
$$\times[v_{j\gamma}(t_{j,l})-u_\gamma(\vec{r}_o,t_{j,l})]\frac{1}{|v_{j\gamma}(t_{j,l})|}. \qquad (12)$$

Next, the intermolecular contribution, $\mathbf{P}^U$, is considered:

$$\mathbf{P}^U(\vec{r},t)=-\frac{1}{2}\sum_j^N\sum_{k(\neq j)}^N \vec{r}_{jk}(t)\vec{\mathbf{F}}_{jk}(t)\int_0^1 d\alpha\,\delta(\vec{r}-\vec{r}_j(t)-\alpha\vec{r}_{jk}(t)).$$

With

$$\int_0^1 d\alpha\,\delta(\vec{r}-\vec{r}_j-\alpha\vec{r}_{jk})=\int_0^1 d\alpha\,\delta(r_\alpha-r_{j\alpha}-\alpha r_{jk\alpha})$$
$$\times\delta(r_\beta-r_{j\beta}-\alpha r_{jk\beta})$$
$$\times\delta(r_\gamma-r_{j\gamma}-\alpha r_{jk\gamma}),$$

we obtain

$$\left\langle\int_0^1 d\alpha\,\delta(\vec{r}-\vec{r}_j-\alpha\vec{r}_{jk})\right\rangle_{\Delta A}$$
$$=\frac{1}{\Delta A}\Omega_1\int_0^1 d\alpha\,\delta(r_{o\gamma}-r_{j\gamma}-\alpha r_{jk\gamma})$$
$$=\frac{1}{2\Delta A}\Omega_1\frac{1}{r_{jk\gamma}}[\mathrm{sgn}(r_{o\gamma}-r_{j\gamma})-\mathrm{sgn}(r_{o\gamma}-r_{k\gamma})],$$

where Ω_1 is defined as

$$\Omega_1=\begin{cases}1, & \text{if there exists } \alpha\in[0,1] \text{ that satisfies}\\ & r_{o\alpha}-\dfrac{\Delta r_\alpha}{2}<r_{j\alpha}+\alpha r_{jk\alpha}(=r_\alpha)<r_{o\alpha}+\dfrac{\Delta r_\alpha}{2} \text{ and } r_{o\beta}-\dfrac{\Delta r_\beta}{2}<r_{j\beta}+\alpha r_{jk\beta}(=r_\beta)<r_{o\beta}+\dfrac{\Delta r_\beta}{2},\\ 0, & \text{otherwise.}\end{cases}$$

We now obtain

$$\tilde{\mathbf{P}}^U_{\gamma\alpha}(\vec{r}_o,t)=-\frac{1}{4\Delta A}\sum_j^N\sum_{k(\neq j)}^N F_{jk\alpha}(t)\Omega_1\{\mathrm{sgn}[r_{o\gamma}-r_{j\gamma}(t)]$$
$$-\mathrm{sgn}[r_{o\gamma}-r_{k\gamma}(t)]\}.$$

We can combine both contributions and obtain an expression for the pressure tensor. It follows that

$$\hat{\mathbf{P}}_{\gamma\alpha}(\vec{r},t)=\frac{1}{\Delta A\tau}\sum_j\sum_{t_{j,l}} m[v_{j\alpha}(t_{j,l})-u_\alpha(\vec{r},t_{j,l})][v_{j\gamma}(t_{j,l})$$
$$-u_\gamma(\vec{r},t_{j,l})]\frac{1}{|v_{j\gamma}(t_{j,l})|}-\frac{1}{4\Delta A\tau}\int_{t-\tau/2}^{t+\tau/2}d\tilde{t}\sum_j^N\sum_{k(\neq j)}^N$$
$$\times F_{jk\alpha}(\tilde{t})\Omega_1\{\mathrm{sgn}[r_\gamma-r_{j\gamma}(\tilde{t})]-\mathrm{sgn}[r_\gamma-r_{k\gamma}(\tilde{t})]\}, \qquad (13)$$

where the subscripts o for $\vec{r}$ and t are omitted. If τ corresponds to a given time step solving the equations of motion, then the integrand in the second term on the right-hand side of Eq. (13) may remain constant, and the operation $(1/\tau)\int d\tilde{t}$ can be removed. It is straightforward to derive the expression for the heat flux vector in a similar manner:

$$\hat{\mathbf{J}}_\gamma(\vec{r},t)=\frac{1}{\Delta A\tau}\sum_j\sum_{t_{j,l}}[v_{j\gamma}(t_{j,l})-u_\gamma(\vec{r},t_{j,l})]U_j(t_{j,l})\frac{1}{|v_{j\gamma}(t_{j,l})|}$$
$$-\frac{1}{4\Delta A\tau}\int_{t-\tau/2}^{t+\tau/2}d\tilde{t}\sum_{j=1}^N\sum_{k=1(\neq j)}^N\vec{\mathbf{F}}_{jk}(\tilde{t})\cdot[\vec{v}_j(\tilde{t})-\vec{u}(\vec{r},\tilde{t})]$$
$$\times\Omega_1\{\mathrm{sgn}[r_\gamma-r_{j\gamma}(\tilde{t})]-\mathrm{sgn}[r_\gamma-r_{k\gamma}(\tilde{t})]\}. \qquad (14)$$

The condition imposed by $\Omega_o\delta(\cdot)$ in Eq. (10) implies that physically, a molecule should be on plane A_o for its action to be counted to the kinetic contribution of the fluxes. In Eqs.

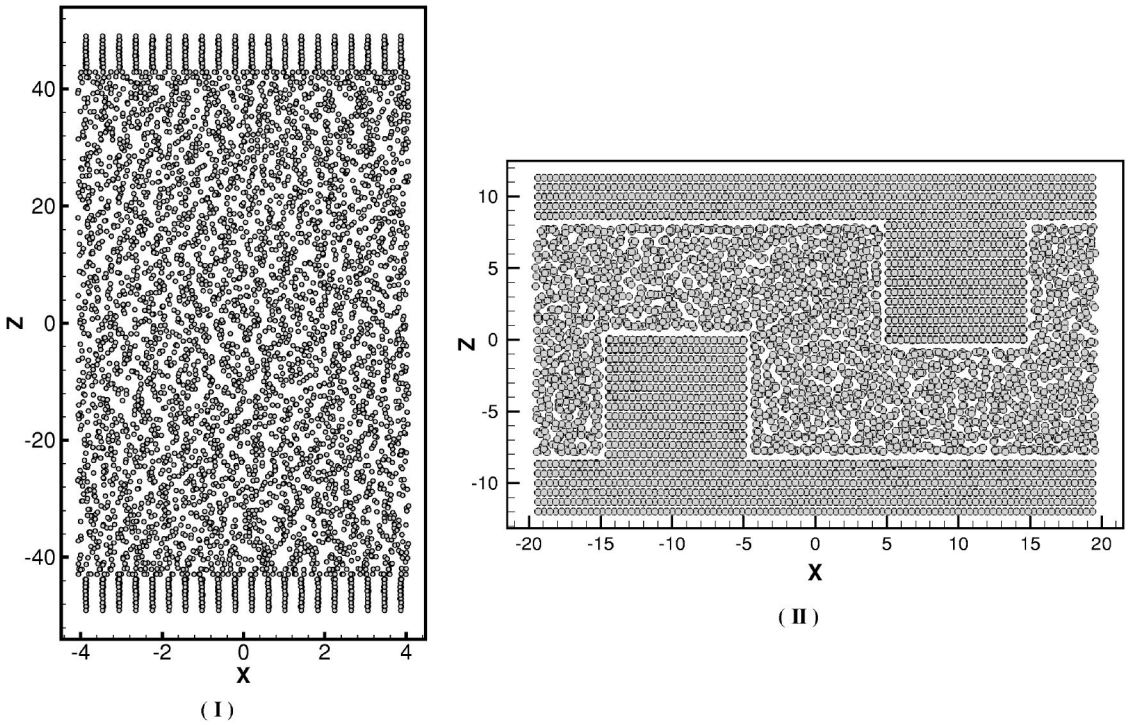

FIG. 1. Snapshots of the simulations. (I) A straight channel with molecularly flat walls. (II) A channel with periodic rectangular turns. The scale of the x, z coordinates is σ.

(13) and (14), $\Omega_1[\mathrm{sgn}(\cdot)-\mathrm{sgn}(\cdot)]$ requires that a point along the line of center of the two molecules should be on plane A_o for their interaction to be included in the potential contribution. These are precisely the flux definitions of Irving and Kirkwood. The bin average implies an average taken over some neighboring planes in the normal direction. The approximation of $O_{ij}\simeq 1$ implies that one of the pairs of interacting molecules must be on the plane for a potential contribution to the fluxes. Both approaches may be a possible source of error, especially for the case of inhomogeneous fluids. It should also be noted that Eqs. (13) and (14) are equivalent to those of MOP, Eq. (5), if the flow is unidirectional, and the fluxes are normal to, and have no gradient in, the flow direction. In this case, the streaming velocity, u_γ, always vanishes. Because the fluxes on A_o centered at $\vec{r}_o$ do not change as $\vec{r}_o$ varies in the streamwise direction, the area can be regarded as being unbounded and $\Omega_{0,1}=1$ can thus be applied all the time.

III. SIMULATIONS

A. Methods

Nonequilibrium molecular dynamics (NEMD) simulations were conducted to determine the pressure and heat transfer using the expressions derived in the above sections. The fluid consists of monatomic molecules that interacts through Lennard-Jones (LJ) 12-6 pairwise potential,

$$u(r) = 4\epsilon\left[\left(\frac{\sigma}{r}\right)^{12} - \left(\frac{\sigma}{r}\right)^{6}\right],$$

where ϵ and σ denote the interaction energy and atomic diameter, respectively, and r is the interatomic distance. The fluid is bounded by two solid surfaces of the (111) planes of an fcc lattice, the number of layers of which was varied: 4 or 5 for case I, 9 for case II, and 13 for the square-shaped humps (see Fig. 1).

A solid atom interacts with the nearest six atoms in the lattice by a harmonic potential of a spring constant, $k=3239.6\epsilon/\sigma^2$ with a nearest neighbor distance of 0.814706σ. The solid atoms interact with the fluid atoms through an LJ potential with $\epsilon_{sf}=16\epsilon$ and $\sigma_{sf}=0.91\sigma$. All the parameters except for the fluid-solid interaction energy were chosen to simulate a system composed of argon and platinum with no electron carriers present [12]. The large value of the fluid-solid interaction energy, ϵ_{sf}, was set for the purpose of minimizing the degree of velocity slip. The solid atoms in the farthest rows of both walls from the fluid side were fixed in space. In the second farthest rows, *ghost* particles are used to set the temperature constant at the boundary of the solid walls (Fig. 2). These observe the Langevin equations, in which parameters from Ref. [12] were used. The equation of motion was integrated according to the velocity Verlet algorithm [13]. The time step was set to $0.0025\sigma\sqrt{m/\epsilon}$. The periodic boundary condition was applied in all three directions.

The measurements were carried out on planes of equal intervals in both the x and z directions. For the kinetic contribution, each particle that crosses a plane is tracked at each step. First, it is checked whether a particle crosses a plane at a given time. Then, the time and velocity at the crossing is calculated using a standard Newton-Raphson algorithm. The internal energy, U_j, for the particle is calculated by interpolating with the values of the four previous time steps [9].

The streaming velocity profile was obtained by collecting and averaging the values of the particles in each bin having

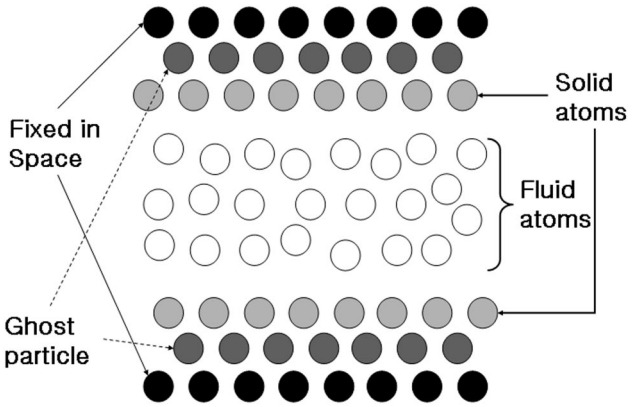

FIG. 2. A schematic drawing of the model system. The number of solid layers was larger in the simulated cases.

the same size as the plane intervals. For the flux measurements, the center of each bin coincides with those of the planes, and the average value in the bin is used as the streaming velocity for the planes that share the center with the bin. For a given arbitrary position on a plane, the velocity was calculated by interpolating the velocities of the plane and two other adjacent planes that share a boundary line with it. It should be noted that the streaming velocity profile was not calculated from the velocity data of particles crossing the planes. The reason for this is as follows. On a plane, the velocities that were collected and averaged were only for particles that crossed the plane. Since the interval between the planes was finite, zero velocity or near-zero velocity particles were seldom on the planes and tended to be discriminated against in the measurements. It is not a problem for the purpose of flux calculations, but it causes a deviation in the streaming velocity. The discriminated values are distributed in a rather symmetric manner about a zero point. If the streaming velocity is also zero, then the errors are largely cancelled out and do not cause any noticeable deviation. If not, however, the mean velocity increases in the absolute value.

At the outset, Eqs. (13) and (14) require both the streaming velocity and each atomic velocity at the crossing at the same time. The former can be obtained only after some time period for averaging. For a long averaging time period, this may cause some technical problems, unless all the phase space data during the simulation can be stored. In Eq. (10), the kinetic component can be arranged into a form where the terms involving the streaming velocity can simply be added. For example,

$$\tilde{\mathbf{P}}^K_{\gamma\alpha} = \frac{1}{\Delta A}\sum_{j=1}^{N} m(v_{j\alpha}v_{j\gamma} - u_\alpha u_\gamma)\Omega_o \delta(r_{j\gamma} - r_{o\gamma}).$$

This addition can be performed after the average is taken at the end of the time period. However, this is not so for Eqs. (13) and (14), where the streaming velocity is nonlinearly related. For a steady-state case, the fluxes may be measured after the mean velocity has been obtained. However, if there are some transient features in the problem, however small, then the serial measurement would induce an error. Therefore, we conducted the same simulations twice using the same initial conditions. The streaming velocity was obtained after the first round simulations, and then, this was used for the fluxes measured in the second round of simulations.

Measurements were also performed simultaneously with the same grid size to compare the approximate formulas (denoted as IK1 in Ref. [8]), which are often used in the literature,

$$\mathbf{P}(\vec{r}_{bin},t) = \frac{1}{V_{bin}}\left\{\sum_{j\in bin} m[\vec{v}_j(t) - \vec{u}(\vec{r}_{bin},t)][\vec{v}_j(t) - \vec{u}(\vec{r}_{bin},t)] - \frac{1}{2}\sum_{j(\in bin)}\sum_{k(\neq j)} \vec{r}_{jk}(t)\vec{F}_{jk}(t)\right\}, \tag{15a}$$

$$\vec{\mathbf{J}}(\vec{r}_{bin},t) = \frac{1}{V_{bin}}\left\{\sum_{j\in bin} [\vec{v}_j(t) - \vec{u}(\vec{r}_{bin},t)]U_j(t) - \frac{1}{2}\sum_{j(\in bin)}\sum_{k(\neq j)} \vec{r}_{jk}(t)[\vec{v}_j(t) - \vec{u}(\vec{r}_{bin},t)]\cdot\vec{F}_{jk}(t)\right\}. \tag{15b}$$

These expressions are based on the previously mentioned approximations and may result in errors. First, the fluid domain was divided into bins in which the data were collected and averaged. That is, this gives averaged values over the volume of the bin. More significant is the use of an approximation for $O_{jk} \simeq 1$. It has been reported that using these leads to spurious fluctuations in the stresses in a liquid-solid interfacial region [8,14]. The same conclusion is drawn in Sec. III B. It is also shown that the approximation leads to a large deviation in the heat flux vector.

B. Results

The fluid flow in two types of channel was considered (Fig. 1). One was a straight channel consisting of two parallel walls of molecularly flat surfaces. The other was a chan-

TABLE I. The parameters for the two simulations.

Case	Domain size [a]	Body force	Grid (x, z)	Temp. [b]	No. of atoms	Time [c]
Straight channel (I)	$8.1\times7.1\times100.8$	0.01	0.19, 0.28	0.7	6000	1000
Periodic turns (II)	$39.1\times7.1\times38.0$	0.5	0.20, 0.19	0.8	10896	3000

[a]The scale of the parameters are as follows: Domain size $=\sigma^3$; body force $=\epsilon/\sigma$; grid $=\sigma$; temperature $=\epsilon/k_B$; time $=\sigma\sqrt{m/\epsilon}$.
[b]The target temperature for the wall boundaries.
[c]The measurement time.

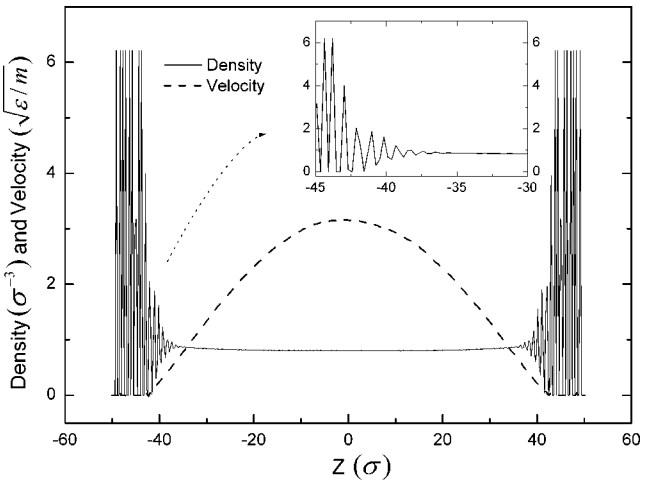

FIG. 3. Density and velocity profiles for the straight channel. The point where the fluid molecules were at the closest distance to the solids, *the contact point*, was about $z=\pm 43\sigma$.

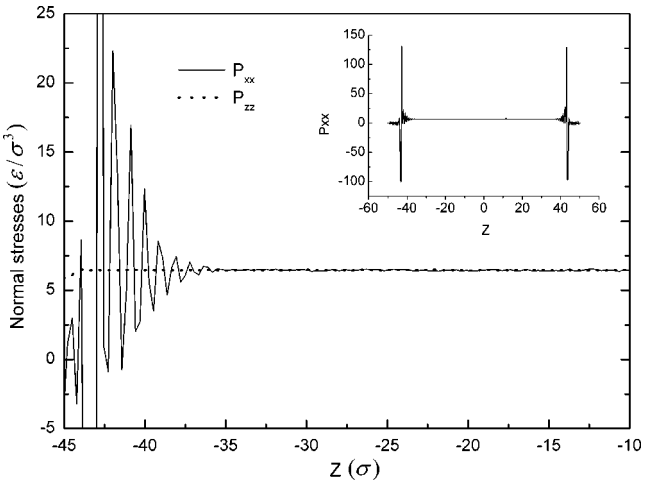

FIG. 4. The normal stresses, P_{xx} and P_{zz}, for the case of a straight channel calculated using Eq. (13).

nel with periodic rectangular turns, where the two walls had periodic *square-shaped humps* alternating by x positions in each wall. An external body force was applied in the $+x$ direction to the fluid atoms in both cases. A unidirectional flow field was developed in the first example, and a more general flow field in the second example. The parameters involved in each case are compared in Table I.

In the first example, an external force of $0.01\epsilon/\sigma$ was applied. After an equilibration period of $1\times 10^3\sigma\sqrt{m/\epsilon}$, a typical Poiseuille flow velocity profile developed, except for small deviations in the region close to the walls. The fluxes were measured on the planes using intervals of 0.19σ and 0.28σ in the x and z directions, respectively, employing Eqs. (13) and (14). The measurements were also performed for bins whose sizes were the same as the intervals used in Eq. (15). The resulting density and velocity profiles are shown in Fig. 3. The point where the fluid molecules make contact or are at the closest distance with the solids is about $z=\pm 43\sigma$. (This distance is referred to as the *contact point* hereafter.) From the contact point to the solid, there is a highly structured region a few molecular diameters thick, and some drastic changes are observed in the measured properties. Higher resolution may be necessary to represent the characteristics of this region more clearly. In this study, we are more concerned about the overall state of the fluid though. In our results, the properties are exhibited well into the solid region for the purpose of continuity in the data. However, the features that largely belong to the solid region are not characterized in detail.

The use of MOP may provide the same results in the case of a unidirectional flow. However, there are additional results that cannot be provided by the MOP technique. These are the fluxes defined on the planes normal to the streamwise direction, such as P_{xx}, P_{xz}, and J_x. These data reveal more features of the dynamic behavior of the fluid flow. The results for the pressure tensors P_{xx} and P_{zz} are shown in Figs. 4 and 5. Since no flow is developed in the z direction, P_{zz} remains constant throughout the fluid domain. It is shown that Eq. (13) resolves the features well throughout this region. The IK1 method also provides good results in the bulk region. However, this does provide some spurious values at the interfacial region, as has been pointed out in the literature [8,14]. This deviation comes from both molecular contributions, kinetic and potential. The kinetic contribution to the deviation may be solely derived using the bin average method, while potential contribution may be derived by approximating O_{jk}, as well as using the average method. This property is shared by all the other components of the stress and heat fluxes in that the results obtained using the IK1 method show significant deviation at the interfacial region. The value of P_{xx} in the bulk has the same value as P_{zz}. It increases in an oscillatory manner as the region nears the solid. While these normal stresses are measured in a nonequilibrium state, it turns out that they are still close to those of the equilibrium state in this particular case. Finally, the value of P_{xz} coincides with the value of P_{zx} in almost all the fluid region (Fig. 6). This reflects the fact that the shear stress is symmetrical, because the fluid is composed of atoms with no internal degrees of freedom. It can also be seen that some

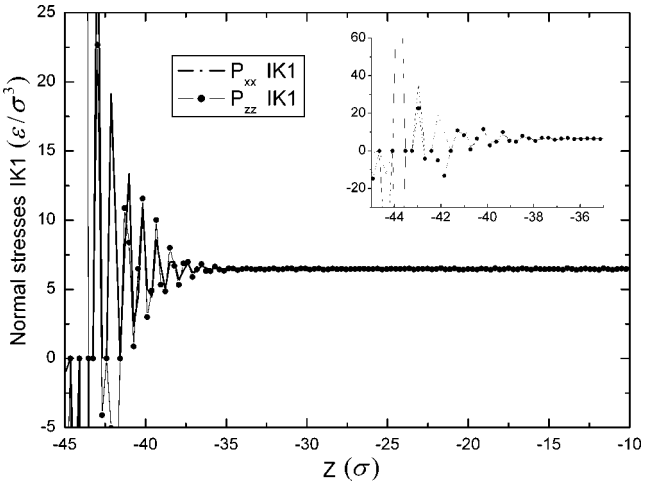

FIG. 5. The normal stresses, P_{xx} and P_{zz}, for the case of a straight channel calculated using the IK1 method [Eq. (15a)].

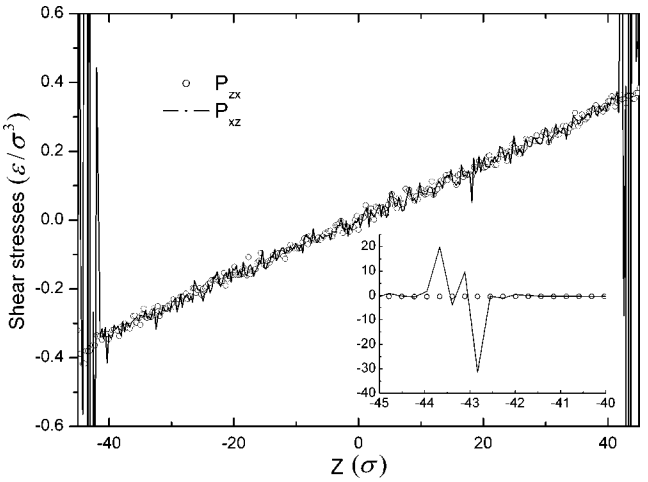

FIG. 6. The shear stresses, P_{xz} and P_{zx}, for the case of a straight channel calculated using Eq. (13).

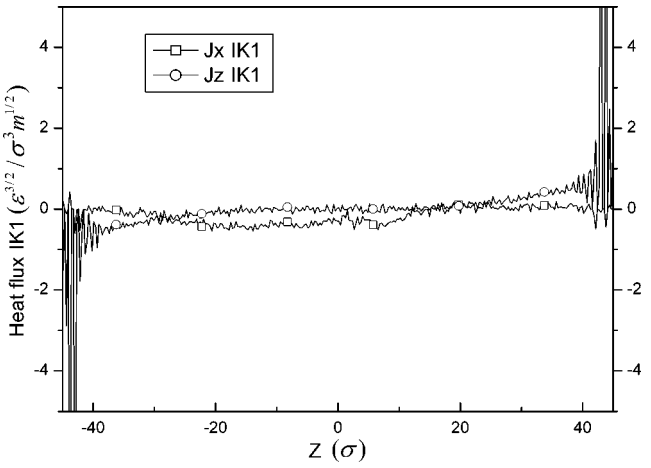

FIG. 8. The heat fluxes, J_x and J_z, for the case of a straight channel calculated using the IK1 method [Eq. (15b)].

structure develops for P_{xz} that deviates from P_{zx} within a distance of one molecular diameter from the contact point.

The measurements of the heat flux in the normal direction also reproduced the trends shown in previous results using the MOP technique (Figs. 7 and 8). That is, in addition to the deviations at the interfacial region mentioned before, a higher level of fluctuations was observed in the heat flux normal to the wall, i.e., J_z, in the IK1 results. Meanwhile, the heat flux in the streamwise direction, J_x, shows marked differences when the two results from Eqs. (14) and (15b) are compared. A significant degree of heat transfer occurs in the upstream direction when measured using Eq. (14), which is missing from the results using the IK1 technique. This difference solely arises from the potential contribution, and it originates from the $\vec{F}_{jk}\cdot[\vec{v}_j-\vec{u}(\vec{r})]$ term. The $[\vec{v}_j-\vec{u}(\vec{r})]$ term is defined in Ref. [9] as the "plane peculiar velocity," which is different from the usual peculiar velocity, $[\vec{v}_j-\vec{u}(\vec{r}_j)]$. In general, the position of particle j for $\vec{v}_j$ does not coincide with that of the mean velocity, $\vec{u}$, on plane $\vec{r}$ (see Fig. 9). In the IK1 method, on the other hand, the positions of the particle and the mean velocity correspond to that of the same bin due to the approximation of $O_{jk}\simeq 1$. The particle velocity can be divided into the mean, or streaming, velocity and the fluctuating velocity, $\vec{v}_j=\vec{u}(\vec{r}_j)+\Delta\vec{v}_j$. Then, the $\vec{F}_{jk}\cdot[\vec{v}_j-\vec{u}(\vec{r})]$ term can be divided into $\vec{F}_{jk}\cdot[\vec{u}(\vec{r}_j)-\vec{u}(\vec{r})]$ and $\vec{F}_{jk}\cdot[\Delta\vec{v}_j-\vec{u}(\vec{r})]$. The former term can make a significant contribution to the heat flux if there is a sizeable gradient in the mean velocity within the range of the intermolecular potential. The results using both methods obey the energy conservation laws for this particular flow, since the continuity equation for energy involves only the divergence of the heat flux vector, which simply vanishes in the unidirectional case. However, Eq. (14) is a more accurate representation of the $\vec{F}_{jk}\cdot(\vec{v}_j-\vec{u})$ term and, therefore, the hydrodynamic equations. This potential source of deviation has already been suggested by Todd *et al.* [9]. In this particular flow, the contribution to J_z is mostly cancelled out, while that to J_x is added together to form a nonzero value (see Fig. 10).

Next, the results for a channel with periodic rectangular turns were considered. Here, the fluid is driven by a stronger force, due to the increased flow resistance from the square-shaped humps. The resulting flow and temperature field are

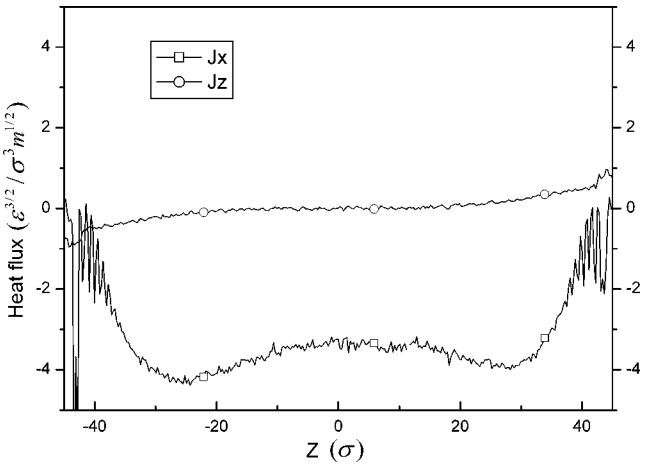

FIG. 7. The heat fluxes, J_x and J_z, for the case of a straight channel calculated using Eq. (14).

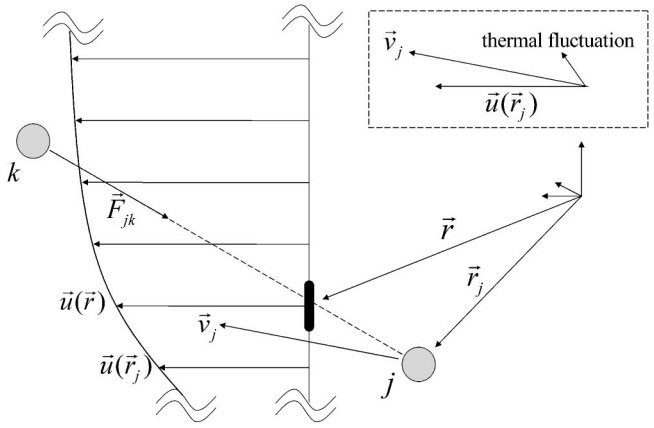

FIG. 9. In the term $\vec{F}_{jk}.[\vec{v}_j-\vec{u}(\vec{r})]$, the position of particle j does not necessarily coincide with that of plane $\vec{r}$. Therefore, in general, the mean velocity of position $\vec{r}_j$ is not the same as that for the plane.

$$J_{x,z} = \ldots + \sum \underbrace{\{F_{jkx}(v_{jx}-u_x)+F_{jkz}(v_{jz}-u_z)\}}_{(1)} \underbrace{\Omega_1\left[Sgn(r_{x,z}-r_{jx,z})-Sgn(r_{x,z}-r_{kx,z})\right]}_{(2)}$$

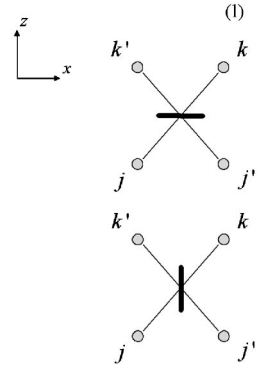

For J_z : $(1)_{jk} = -(1)_{j'k'}$; $(2)_{jk} = (2)_{j'k'}$

For all cases,

$$\begin{cases} F_{jkx} = -F_{j'k'x}; \; u_x(r_j) = u_x(r_{j'}), \\ F_{jkz} = -F_{j'k'z}; \; u_z(r_j) = u_z(r_{j'}) = 0. \end{cases}$$

For J_x : $(1)_{jk} = -(1)_{j'k'}$; $(2)_{jk} = -(2)_{j'k'}$

FIG. 10. When the unidirectional flow in Fig. 3 is considered, there is no gradient in the properties in the x direction. Therefore, there are equal probabilities for the pairs jk and $j'k'$ occurring. The contributions of these pairs to the heat flux are cancelled out for J_z, but superposed for J_x.

shown in Fig. 11, and a more general flow structure developed. No noticeable unstable features were observed in the calculations, and a large velocity slip on the wall occurs, due to the relatively strong driving force. Large values in the temperature distribution occur due to a similar reason.

Again, the energy input by the force is turned into heat by viscous dissipation inside the fluid, and this is transferred to the walls. A lower temperature is observed in regions of stagnant flow or lower velocity gradients. The fluxes were measured on the planes using Eqs. (13) and (14). A much larger number of samples than normal was required to maintain the same degree of resolution and accuracy as in the previous example. A grid size of 0.20σ and 0.19σ was used for the x and z directions, respectively. The calculations were carried out for $3000\sigma\sqrt{m/\epsilon}$. The normal stresses in the tangential direction to the solid surface show large gradients in the

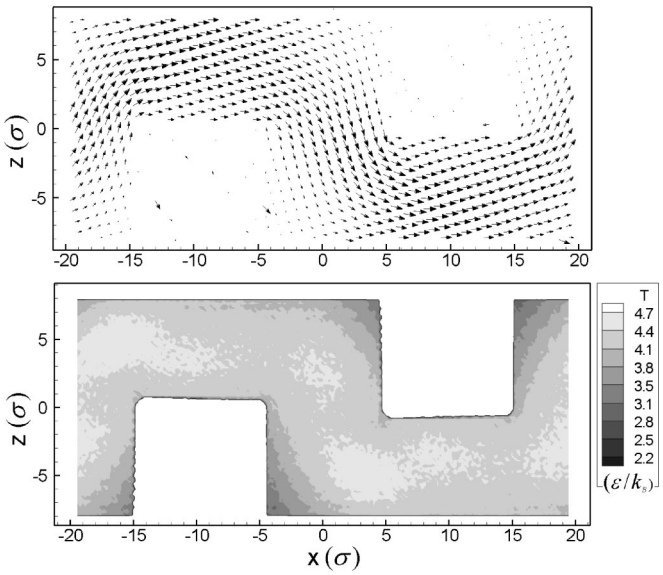

FIG. 11. The velocity field (upper graph) and the temperature distribution (lower graph) for a channel with periodic rectangular turns.

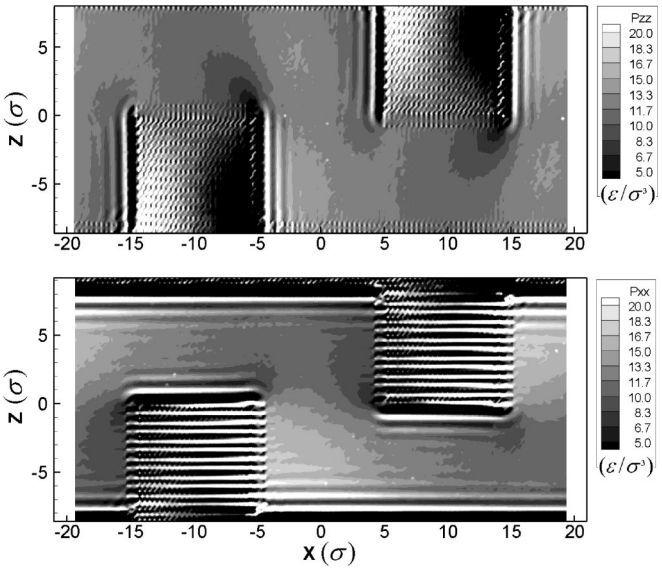

FIG. 12. The normal stresses for the case of a channel with periodic rectangular turns. The upper graph shows data for P_{zz} and the lower graph shows data for P_{xx}. These were calculated using Eq. (13).

region very close to the walls (Fig. 12). This is because the density is highly varied, and the flow is restricted in the normal direction. The stress in the normal direction to the main flow maintains a constant value. Larger gradients are shown near the edges, where marked turns in the flow streams occur. Accordingly, large concentrations of the shear

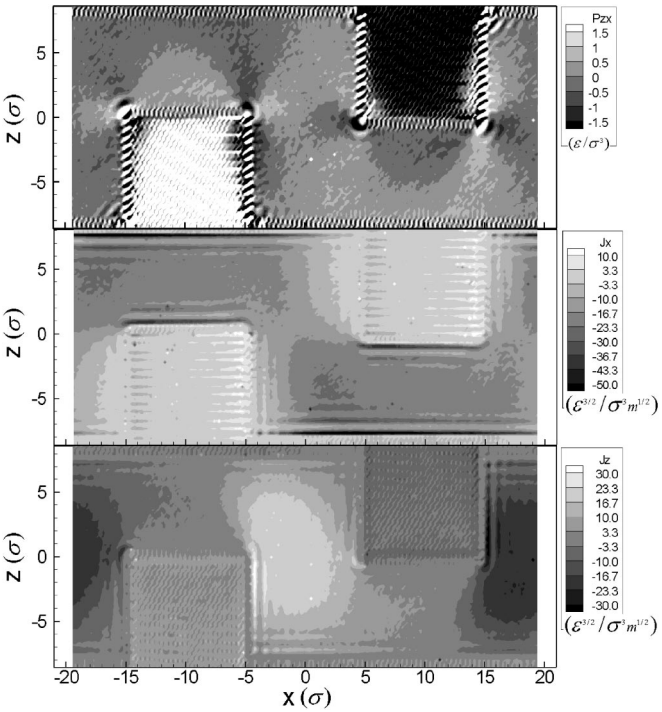

FIG. 13. The shear stress and heat fluxes for a channel with periodic rectangular turns. The uppermost graph shows data for P_{zx}, the middle graph shows data for J_x, and the lower graph shows data for J_z. These were calculated using Eqs. (13) and (14).

stress is observed there (Fig. 13). The values of P_{xz} and P_{zx} are the same as those of the previous example.

Finally, the heat fluxes are similarly formed from inside the fluid to the walls, and increase as it nears the walls (Fig. 13). There also exists significant heat flux in the upstream direction, as in the previous case. On the whole, the features found in the unidirectional flow example are still observed regionally. In addition, we observed the features that are found only in the general geometry case, such as stress concentrations near edges and flux gradients parallel to the flow.

IV. CONCLUSIONS

We have developed a method for calculating the heat and momentum fluxes of a fluid in a general state. The method can be used for resolving the state of a highly inhomogeneous fluid away from equilibrium. This is a strong point of the method shared with the method of planes approach. However, the latter method is only relevant for the flow of simple geometries, and only provides part of the flux components. Our expression can be applied to general flows, and affords the remaining components that are not provided by the MOP.

The flux expressions are derived from the definitions of instantaneous fluxes, which satisfy the conservation equations at a given moment and, therefore, are valid in the nonequilibrium state. Two approximate approaches that are in common use are not adopted: the $O_{jk} \simeq 1$ approximation, and coarse graining in space. First, the term involving the O_{jk} operator is replaced by an equivalent in an integrated form useful in avoiding the approximation. Next, the fluxes are measured on planes, and a time-average value is adopted to avoid the average in the extra space dimension. The final expressions, Eqs. (13) and (14), correspond to the original flux definition of Irving and Kirkwood, and they are equivalent to the MOP if the flow is unidirectional, and the fluxes are normal to, and have no gradient in, the flow direction.

The NEMD results for unidirectional flow show that the IK1 expressions, Eq. (15), is a poor representation of the inhomogeneous state, which agrees with previous studies. Our method provides additional flux components defined in the planes normal to the streamwise direction. It reveals that there is a significant degree of heat flux in the upstream direction. This is new information that is not provided by the MOP and is missing in results using the IK1 method. This is due to the so-called "plane peculiar velocity," $\vec{v}_j - \vec{u}(\vec{r})$, which is different from the peculiar velocity, $\vec{v}_j - \vec{u}(\vec{r}_j)$. The potential part of the heat flux contains the plane peculiar velocity in the form of $\vec{\mathbf{F}} \cdot [\vec{v}_j - \vec{u}(\vec{r})]$, where the position of particle j does not necessarily coincide with the plane position, $\vec{r}$. On the other hand, the IK1 method collects the potential contribution in such a way that the two positions correspond to the same bin, and, as in the case of a nanoscale-width channel, the flow with a sizeable gradient within the range of the molecular potential may result in a significant deviation in heat flux using the IK1 method. Equations (13) and (14) are also applied to a more general geometry of a channel with periodic rectangular turns. These results agree with those of the unidirectional case when the flow becomes regionally unidirectional. Three-dimensional features were also resolved, such as the stress concentrations near edges, and the flux gradients parallel to the flow.

ACKNOWLEDGMENT

We gratefully acknowledge that this work was supported by Micro Thermal Research Center.

[1] D. A. McQuarrie, *Statistical Mechanics* (Harper Collins, New York, 1976).
[2] J. Irving and J. G. Kirkwood, J. Chem. Phys. **18**, 817 (1950).
[3] D. J. Evans and G. P. Morriss, *Statistical Mechanics of Nonequilibrium Liquids* (Academic, London, 1990).
[4] A. Harasima, Adv. Chem. Phys. **1**, 203 (1958).
[5] P. Schofield and J. Henderson, Proc. R. Soc. London, Ser. A **379**, 231 (1982).
[6] B. Hafskjold and T. Ikeshoji, Phys. Rev. E **66**, 011203 (2002).
[7] E. Wajnryb, A. R. Altenberger, and J. S. Dahler, J. Chem. Phys. **103**, 9782 (1995).
[8] B. Todd, D. J. Evans, and P. J. Daivis, Phys. Rev. E **52**, 1627 (1995).
[9] B. Todd, P. J. Daivis, and D. J. Evans, Phys. Rev. E **51**, 4362 (1995).
[10] O. G. Jepps and S. K. Bhatia, Phys. Rev. E **67**, 041206 (2003).
[11] T. Qian, X.-P. Wang, and P. Sheng, Phys. Rev. E **68**, 016306 (2003).
[12] S. Maruyama and T. Kimura, Int. J. Heat Technol. **18**, 69 (2000).
[13] M. Allen and D. Tildesley, *Computer Simulation of Liquids* (Clarendon, Oxford, 1987).
[14] F. Varnik, J. Baschnagel, and K. Binder, J. Chem. Phys. **113**, 4444 (2000).
[15] J. Cormier, J. Rickman, and T. Delph, J. Appl. Phys. **89**, 99 (2001).
[16] A different route to the relationship may be available by using Fourier space (see Ref. [15]).